

Article

Optimal Power Flow of Integrated Renewable Energy System using a Thyristor Controlled Series Compensator and a Grey-Wolf Algorithm

M. Rambabu ¹, G. V. Nagesh Kumar ^{2,*} and S. Sivanagaraju ³

¹ Department of EEE, GMR Institute of Technology Rajam, Rajam, AP 532127, India; m.rambabu2001@gmail.com

² Department of EEE, JNTUA CE Pulivendula, Pulivendula, AP 516390, India

³ Department of EEE, JNTUK Kakinada, Kakinada, AP 533001, India; sirigiri70@gmail.com

* Correspondence: gundavarapu_kumar@yahoo.com

Received: 16 April 2019; Accepted: 30 May 2019; Published: 11 June 2019



Abstract: In recent electrical power networks a number of failures due to overloading of the transmission lines, stability problems, mismatch in supply and demand, narrow scope for expanding the transmission network and other issues like global warming, environmental conditions, etc. have been noticed. In this paper, a thyristor-controlled series compensator (TCSC) is placed at the optimum position by using two indices for enhancing the power flows as well as the voltage security and power quality of the integrated system. A fused severity index is proposed for the optimal positioning along with a grey wolf algorithm-based optimal tuning of the TCSC for reduction of real power losses, fuel cost with valve-point effect, carbon emissions, and voltage deviation in a modern electrical network. The voltage stability index to evaluate the power flow of the line and a novel line stability index to assess the line capacity are used. The TCSC is placed at the highest value of the fused severity index. In addition, an intermittent severity index (IMSI) is used to find the most severely affected line and is used for relocating the TCSC to a better location under different contingencies. Lognormal and Weibull probability density functions (PDFs) are utilized for assessing the output of photovoltaic (PV) and wind power. The proposed method has been implemented on the IEEE 57 bus system to validate the methodology, and the results of the integrated system with and without TCSC are compared under normal and contingency conditions.

Keywords: indices; grey wolf optimization; solar; wind; generator reallocation; distribution functions; TCSC

1. Introduction

In the recent past interest in distributed generation has increased tremendously due to the cost of fuel, carbon footprint concerns, load demand, and its delivery of clean power, etc. At present, the electrical power system is facing various problems like network communication, load demand, environmental constraints and limited expansion of lines that influence the sustainability and reliability. These issues have encouraged researchers to utilize solar and wind generation for the reduction of transmission losses, carbon emissions and fuel cost. These sources can be operated either in private or grid-connected modes. The idea of wind and solar associated with a conventional system, though innovative, has caused more difficulties for planners and analysts due to the need to improve voltage stability and sustainability. Researchers are searching for better strategies to utilize the maximum power within the predefined conditions. This development can be possible by associating shunt and series devices and keeping voltages within specified limits. Lately, the improvement of power

electronic devices provide control and is adaptable to FACTS. FACTS instruments can be utilized to control various parameters of the transmission lines in a powerful way. The capacity of these devices can be used appropriately by properly tuning and placement at a specific location in the network and this leads to the reduction of active power losses and maintains stability. Various optimization methods have been proposed for obtaining the desired system performance.

In the literature, various distributed generation systems like wind, solar, etc. combined with conventional thermal generators are proposed to alleviate many of the concerns [1–8]. Abaci et al. [9] clarified the planning of generators considering the monetary criteria, values of shunt capacitors, load tap changers in the OPF outline. Shi et al. [10] have talked about and reviewed diverse systems utilized with OPF under wind power constraints and environmental cost benefits. Sichilalu et al. [11] have endeavored to consolidate a heat pump-based water heater model which is delivered by wind and a PV solar system considering price minimization and electricity tariff as an objective. Levron et al. [12] demonstrated control of stored energy to balance the power generation by renewable energy sources. Biswas et al. [13] have demonstrated some vulnerabilities of PV and wind, where the constraints are incorporated with conventional generators for the objective function. Reserve cost, penalty cost, and estimated cost of renewable energies are additionally considered for taking care of the OPF issue.

Hamzeh Aghdam et al. [14] demonstrated that line blackouts due to the failure of system components, overburden, and high infiltration of renewable energy sources might influence the entire energy management of the system. Rao et al. [15] clarified the optimum placement for SVC utilizing firefly and BAT algorithms. Hingorani et al. [16] explained and analyzed various devices for different types of electrical power system issues. Bali et al. [17] proposed a combined index-based optimal generation reallocation utilizing a harmony search algorithm. Kumar Gundavarapu et al. [18] recommended a disparity line-based utilization index for the ideal location of interline power flow controllers based on the resolution of line flows using a firefly algorithm. Modarresi et al. [19] have demonstrated various indices suitable for finding the frail lines and buses for optimal placement problems. Kim et al. [20] explained the available transfer capability for the power flow using the fuzzy sets. Nireekshana et al. [21] investigated the use of TCSC, SVC to enhance the power transfer capability using a cat swarm algorithm. Mansour et al. [22] proposed optimal placement for TCSC under the condition of voltage stability. Bhattacharyya et al. [23] demonstrated the optimal TCSC location aimed at the enhancement of power flow by setting the control parameters like generator outputs, tap changing transformers, etc. Over the last two decades, many metaheuristic algorithms have been developed. Some of them are utilized for the optimal power flow problems for various applications and objectives considering equality and inequality constraints. The novel algorithms used for optimum power flow include the krill herd procedure [24], particle swarm optimization (PSO) [25], adaptive group search optimization procedure [26] for multi-tasking functions. Mirjalili et al. [27] demonstrated a new meta-heuristic grey wolf algorithm in 2014 which provides the best results as compared to existing optimizing methods.

This paper predominantly focuses on optimal power flow-based generation reallocation of a renewable integrated power system in the absence and presence of TCSC utilizing a grey wolf algorithm. A fused severity factor that is a blend of a rapid voltage stability index (RVSI) and a novel line stability index (NLSI) has been framed to achieve the optimum position of the TCSC device and is additionally utilized to attain a precise measurement of overburdened lines. RVSI is being used for the assessment of loaded lines concerning line parameters and reactive power. NLSI is used for the estimation of the overloaded line concerning real power and resistance. FSI is determined to find the frail lines connected to the buses of the power system. Every one of the lines is positioned in descending order based on the fused severity index. The line sets that have the maximum value of FSI are reviewed as optimum placement locations for TCSC. The multi-objective task consists of active power loss, carbon emission, voltage deviation and fuel cost with valve-point impact has been formulated for optimum tuning of TCSC using grey wolf optimization. A detailed assessment of the results has been compared to an

IEEE 57-bus system to mark the effectiveness of the proposed model. It is also verified for different conditions like normal loading and contingency conditions.

2. Problem Design

The main objective is to decide the generation reallocation and optimum parameter of the integrated energy system. The objective function is explained as below.

2.1. Objective Function

A multi task function is formulated and given as the following equations:

$$\text{Min}F = \text{Min} (w_1 * F_C + w_2 * F_{VPE} + w_3 * F_{PL} + w_4 * F_{VD} + w_5 * F_{CE}) \quad (1)$$

$$w_1 + w_2 + w_3 + w_4 + w_5 = 1 \quad (1a)$$

$$w_1 = w_2 = w_3 = w_4 = w_5 = 0.2 \quad (1b)$$

Weightage of individual objective task has given equal priority and the total is equal to one. F_C , F_{VPE} , F_{PL} , F_{VD} , F_{CE} are the different individual objective functions explained as follows.

2.1.1. Real Power Generation Cost

This cost function can be minimized utilizing the accompanying quadratic condition:

$$F_{C1} = \text{Min} \left(\sum_{i=1}^{N_{TG}} a_i + b_i P_{TGI} + C_i P_{TGI}^2 \right) \quad (2)$$

$$F_{we}(P_{we}) = g_e P_{we} \quad (3)$$

$$F_{sf}(P_{sf}) = h_f P_{sf} \quad (4)$$

$$F_c = F_{c1} + F_{we} + F_{sf} \quad (5)$$

2.1.2. Real Power Generation Cost with Valve-Point Effect

$$F_{VPE}(P_{TG}) = \sum_{i=1}^{N_{TG}} a_i + b_i P_{TGI} + C_i P_{TGI}^2 + |d_i \times \sin(e_i \times (P_{TGI}^{min} - P_{TGI}))| \quad (6)$$

The valve-point loading impact has been considered on account of the fact it allows more operative and accurate modeling of cost functions. By studying the effect of multi-valve turbines, the power system displays more significant variation in the generating cost and sinusoidal function is upgraded to the fuel cost.

2.1.3. Active Power Loss

This objective comprises minimizing the active power losses in a transmission line. This can be represented as:

$$F_{PL} = \text{min}(P_{Loss}) = \text{min} \left(\sum_{k=1}^{nl} \text{real}(S_{ij}^k + S_{ji}^k) \right) \quad (7)$$

2.1.4. Voltage Deviation

Voltage deviation (VD) is considered is to attain the required transmission voltage of a given system and can be expressed as:

$$F_{VD} = \min(VD) = \min\left(\sum_{k=1}^{N_{bus}} : V_k - V_k^{ref} :^2\right) \quad (8)$$

2.1.5. Emission

With an increase in the polluting environment, it is desirable to take the emissions into account to modify the optimal power flow. The total ton per hour emissions of the environmental pollutants caused by thermal units can be represented as follows:

Emission in tons per hour (ton/h) is calculated by:

$$F_{CE} = \sum_{i=1}^{N_{TG}} [(\delta_i + \varphi_i P_{TG_i} + \lambda_i P_{TG_i}^2) \times 0.01 + \psi_i e^{(\sigma_i P_{TG_i})}] \quad (9)$$

2.2. Modeling of Installed TCSC

The active and reactive power equations at bus t are:

$$P_t = V_t V_m B_m \sin(\theta_t - \theta_m) \quad (10)$$

$$Q_t = V_t^2 V_m B_m \cos(\theta_t - \theta_m) \quad (11)$$

2.3. Equality Constraints

Power balance Equations:

$$\sum_{i=1}^N P_{Gi} = \sum_{i=1}^N P_{Di} + P_L \quad (12)$$

$$\sum_{i=1}^N Q_{Gi} = \sum_{i=1}^N Q_{Di} + Q_L \quad (13)$$

$$\text{where : } P_{Gi} = \sum_{j=1}^N P_{Gj} + P_{we} + P_{sf} \quad (14)$$

2.4. Inequality Constraints

2.4.1. Voltage Limits for Generator Buses

$$V_{Gi}^{min} \leq V_{Gi} \leq V_{Gi}^{max} \quad (15)$$

2.4.2. Real Power Generation Limits

$$P_{Gi}^{min} \leq P_{Gi} \leq P_{Gi}^{max} \quad (16)$$

where $G_i = 1, 2, 3, \dots, n_{gb}$ and n_{gb} = overall number of generator buses.

2.4.3. Reactive Power Generated Limits

$$Q_{Gi}^{min} \leq Q_{Gi} \leq Q_{Gi}^{max} \quad (17)$$

2.4.4. TCSC Limits

$$X_{TCSC}^{min} \leq X_{TCSC} \leq X_{TCSC}^{max} \quad (18)$$

2.4.5. Wind Power Constraint

$$P_{we}^{min} \leq P_{we} \leq P_{we}^{max} \quad (19)$$

2.4.6. Solar PV Power Constraint

$$P_{sf}^{min} \leq P_{sf} \leq P_{sf}^{max} \quad (20)$$

3. Index Based on Optimal Placement of TCSC

3.1. Rapid Voltage Stability Index

To assess the voltage stability of an electrical power network, a rapid voltage stability index (RVSI) is taken to indicate a system's weakness and susceptibility to voltage collapse [28]:

$$RVSI_{ij} = 4 \frac{X_{ij}}{V_i^2} \left(\frac{P_j^2}{Q_j} + Q_j \right) \quad (21)$$

$RVSI_{ij}$ = RVSI for the line associated with bus i and bus j . A heavily loaded line has a RVSI magnitude close to unity. Hence, RVSI values are kept at less than unity to ensure system stability.

3.2. Novel Line Stability Index

To determine the congestion of transmission lines and line capacity utilization, a novel line stability index (NLSI) is taken as [29]:

$$NLSI_{ij} = \frac{R_{ij}P_j + X_{ij}Q_j}{0.25V_i^2} \quad (22)$$

NLSI gives an estimate of the percentage of the line being utilized.

3.3. Fused Severity Index

A fused index is formulated as a combination of NLSI and RVSI index set by the following balanced equation:

$$FSI = m1 \times NLSI + m2 \times RVSI \quad (23)$$

where $m1 = m2 = 0.5$.

3.4. Intermittent Severity Index

After performing the contingency analysis, the intermittent severity index (IMSI) is determined to find a better location for the placement of TCSC. In this analysis, primarily the highest value of FSI for a specific line among all line contingencies is determined. Then the number of times that line has been repeated in the line outages is identified. Lastly, the value of IMSI for a particular line can be obtained by multiplying the maximum value of FSI of that line for different line outages and the number of times that particular line has appeared in the severity list. The same procedure is repeated for all the lines. The line that is having the highest value of IMSI is considered as the most severe line:

$$IMSI_{ij} = PB_{ij} \times FSI_{ij}^{MAX} \quad (24)$$

$IMSI_{ij}$ and FSI_{ij}^{MAX} are intermittent severity index and maximum fused severity index of the line between the i -th and j -th bus.

4. Weibull and Lognormal for Wind/PV

To assess the output power of wind, the Weibull PDF is used. In the Weibull study, the frequency, probability and cumulative probability are determined. The complete procedure of the Weibull PDF is given below.

4.1. Weibull PDF

Here, the wind speed distribution is measured to utilize the Weibull PDF. In the Weibull, two parameters are used. The primary one is a scale constraint, and the second one is a shaped constraint. For the analysis of wind speed, the following Weibull distribution formula is given as:

$$f(v) = \frac{k}{c} * \left(\frac{v}{c}\right)^{k-1} * e^{-\left(\frac{v}{c}\right)^k} \quad (25)$$

where c and k denote the wind speed characteristics. If the c value is less the wind speed is also less. After that, the cumulative Weibull distribution is calculated by the succeeding function:

$$F(v) = 1 - e^{-\left(\frac{v}{c}\right)^k} \quad (26)$$

Based on that, the cumulative Weibull distribution function is calculated, later the frequency is resolved. The wind power energy can be acquired by employing its power curve and represented by the succeeded equation:

$$P(v) = \begin{cases} 0 & v < v_{ci} \text{ or } v > v_{co} \\ q(v) & v_{ci} \leq v \leq v_r \\ P_r & v_r < v < v_{co} \end{cases} \quad (27)$$

Similarly, the lognormal function is examined for the PV power generation.

4.2. Lognormal PDF

In the section, the lognormal PDF function is used for the analysis of power in PV with random variable x . Lognormal distribution equation is given below with standard deviation and the mean:

$$f(x : \mu, \beta) = \begin{cases} \frac{1}{\beta x \sqrt{2\pi}} e^{-\frac{1}{2\beta^2} [\ln(x) - \mu]^2} & x \geq 0 \\ 0 & \text{Otherwise} \end{cases} \quad (28)$$

The density function for the analysis is represented as:

$$r(x) = \frac{1}{x\beta\sqrt{2\pi}} e^{-\frac{[\ln(x)-\mu]^2}{2\beta^2}} \quad (29)$$

The mean and variance of the lognormal distribution is calculated as the following equation:

$$\mu = e^{\mu + \frac{\beta^2}{2}} \quad (30)$$

$$\beta^2 = e^{2\mu + \beta^2} (e^{\beta^2} - 1) \quad (31)$$

The lognormal distribution is used for an extensive assortment of applications. It applied and assessed the output power of PV. Based on that, the frequency and probability of PV are analyzed. Here, the mean and variance values are changed; the relating values are assessed. The lognormal based PV is utilized to analyze the output power. After that, the variation of the mean and covariance parameters, the output power is resolved and accomplishes the optimal power flow solutions.

5. Optimal Tuning of TCSC using Grey Wolf Optimization

Mirjalilidescribed the grey wolf optimizer (GWO)algorithm in 2014 [27]; this procedure is wholly structured dependent on seeking prey and individual chasing agents of grey wolves. In this technique, four unique dimensions of chains of hierarchies are present. Grey wolves including ‘p’ being first then followed by the second one ‘q’ then third one ‘r’ and the last dimension ‘s.’Grey wolves are increasingly keen on living in a gathering. The pack size might be overall of around 5–12 wolves. Figure 1 depicts the flow chart for multi-objective function utilizing the grey wolf algorithm.

Algorithm 1. Grey Wolf Optimizer (GWO) Algorithms

1. Generate the initial prey wolf population/search agents
 Y_j (where $j = 1, 2 \dots n$)
 2. Initialize a, A and C
 3. Compute the fitness value of each search agent
 Y_α = the best seek after an authority
 Y_β = the second best seek after an authority
 Y_δ = the third best seek after an authority
 4. Initialize Iteration = 1
 5. Repeat the steps
 6. For $j = 1$: Y_s (size of Grey wolf)
For each chase agent
Invigorate the location of the current chase agent by using the equation
 $Y(k+1) = Y1 + Y2 + Y3/3$
End for
 7. Compute the fitness values of all chase agents
 8. Renew the vectors of a, A and C
 9. Renew the values of $Y_\alpha, Y_\beta, Y_\delta$
 10. Increment the Iteration ($k = k+1$)
 11. While (iterations < max number of iterations)
 12. Get the output Y_α
-

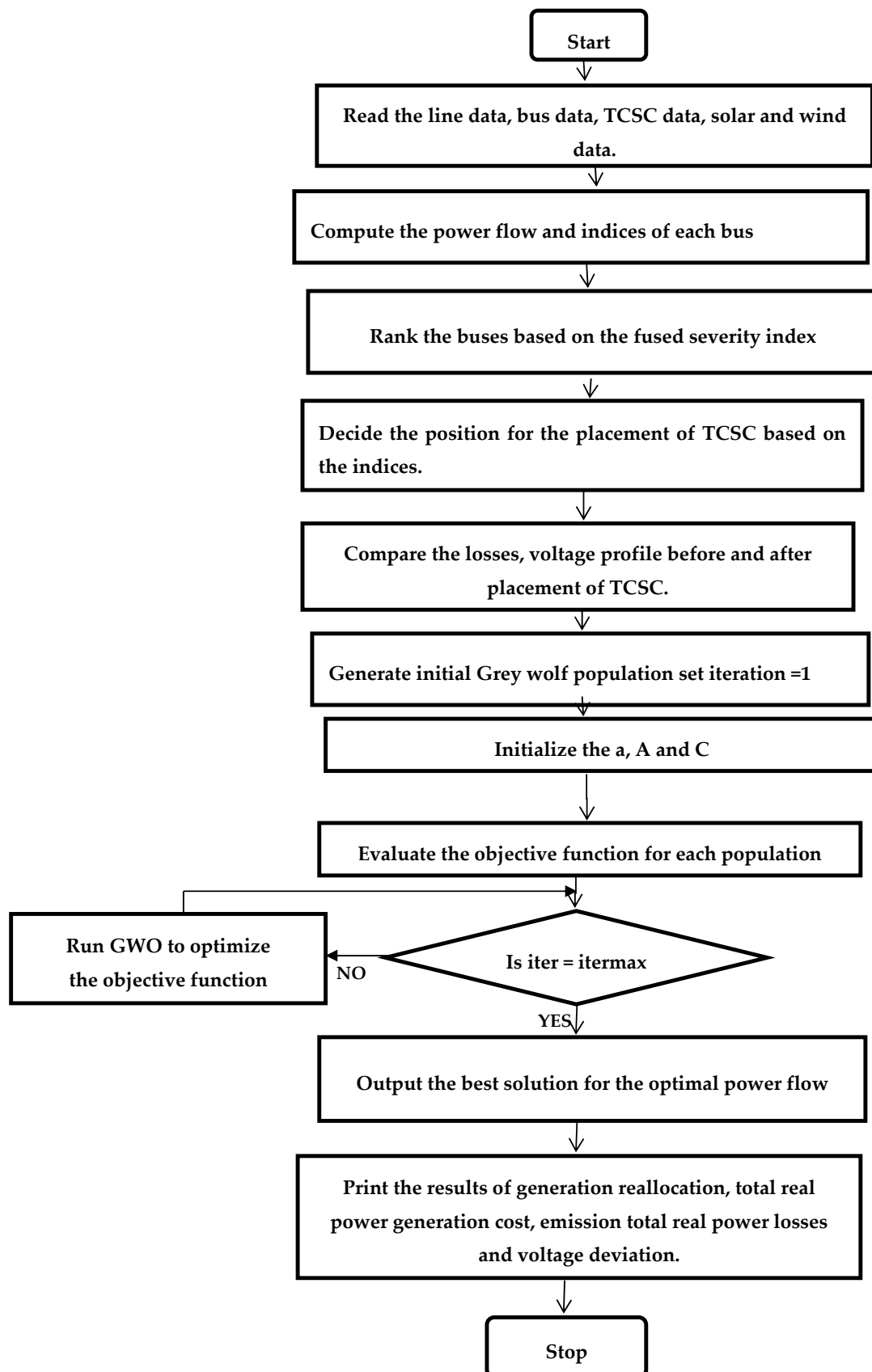


Figure 1. Flow chart for multi-objective optimization using grey wolf algorithm.

6. Simulation Results

An IEEE 57 bus system is amended to incorporate renewable energy system with equivalent values of thermal Generators. The grey wolf technique is used to resolve the OPF problem and check the effectiveness of the suggested method. Here 24h data is considered for the solar and wind power analysis [30]. The actual output power of the wind turbine is determined by using Weibull PDF and its variations of speed are noted. The wind speed is assumed as the miles per hour (m/h) and then it is converted into m/sec. Based on the Weibull PDF, the frequency is analyzed and plotted in Figure 2. Here, the output power flow of PV is investigated with the help of lognormal PDF functions. One PV is employed and the 24h PV data is noted. Based on the data, the irradiance level is noted and the corresponding frequency is determined and illustrated in Figure 3. The mean output power values of the wind farm and solar is assumed for solving the OPF and the proposed grey wolf algorithm has been implemented on IEEE-57bus system in the presence and absence of TCSC. Moreover, different cases like normal loading and contingency have been investigated and reported in separate tables to support the proposed method.

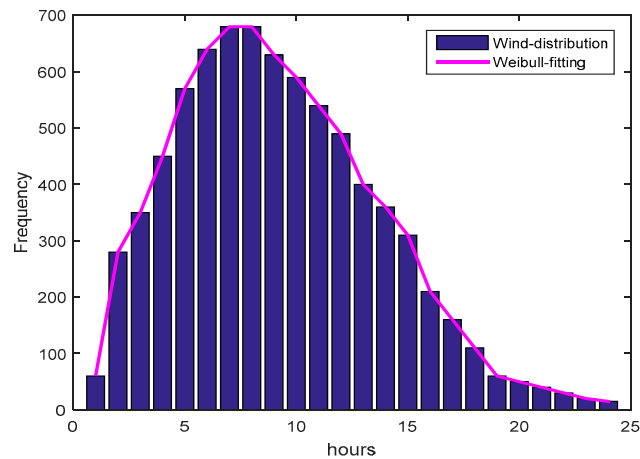


Figure 2. Frequency analysis-based wind speed ($k = 3$, $c = 6$).

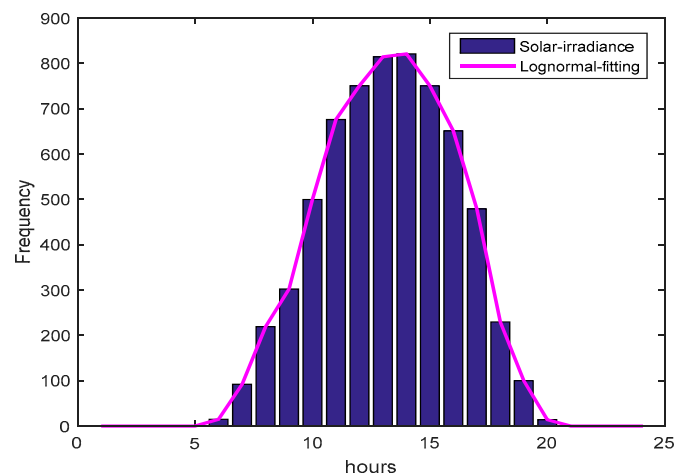


Figure 3. Illustrations of frequency for solar (mean = 2, SD = 3) variation.

6.1. IEEE57 BusTest System

The modified IEEE 57 bus test system comprises of seven generators, among them slack bus is placed at bus 1 and four thermal generators are placed at the buses nos. 2,3,6,8, the solar system is located at bus 9 and wind system is located at bus no. 12 and the remaining 50 buses are treated as load

buses. This configuration has 80 interconnected lines. The generator cost coefficient characteristics of IEEE57 bus have been presented in the Appendix A. Only load buses are assumed for the optimal placement of TCSC. Grey wolf optimization is utilized for obtaining the optimal power flow including and excluding TCSC and program is executed in MATLAB software and parameters are tabulated. Equal weights of 0.2 have been considered for all objectives. The results are carried out for different objective function. The Enercon model E82-E4 wind farm is chosen as the model connected to bus 12 and its datasheet is taken as reference for the analysis. The different speed values taken are $v_{in} = 3$ m/s, $v_r = 12$ m/s and $v_{out} = 25$ m/s. Here 120 wind turbines, each with a rating of 3 MW are considered to form a wind farm of 360 MW rating which gives a maximum output of 212 MW according to the Betz law. This value is taken as output power of the wind farm. Solar park of 200 MW is considered for the radiation of 800 w/m^2 in the standard climatic conditions. Table 1 represents the parameters of the grey wolf algorithm.

Table 1. Grey wolf algorithm parameters.

Serial Number.	Parameters	Quantity
1	Grey wolf size	20
2	Number of iterations	50
3	a vector	2

6.2. Normal Loading Condition

The different arrangements of weights related to NLSI and RVSI are altered and the obtained values are listed in Table 2. As the weighted values are changing the FSI value is decreasing. The weighted factors demonstrate the necessity of indices. The total value of NLSI is more than the value of the total value of NVSI further decrease in values is not desirable minimum values of total fused severity index has been observed for $m_1 = -0.5$ and $m_2 = 0.5$ and equal priority of indices has been selected for the calculations. Figure 4 shows NLSI, RVSI, FSI values for totally ranks of IEEE 57 bus system. Table 3 indicate that the top 25 RVSI, NLSI, and FSI values of all severity lines are listed in decrease order. From Table 3, it is noticed that line 56 connected between buses 41–43 has the highest FSI value. This location was chosen for the optimal placement for the TCSC based upon the highest fused severity index values. An additional node 58 is considered in between 41 and 43 for TCSC placement, and it is observed that losses, carbon emissions, fuel cost with valve-point effects are reduced at that particular location as compared to the placing TCSC at different positions of the IEEE 57 bus system as tabulated in Table 4. The system is tuned with a grey wolf algorithm by comprising the objective functions like generation fuel cost, active power losses, carbon emissions, fuel cost with valve-point effect and voltage deviations with and without TCSC. Tables 5 and 6 indicate the different individual as well as multi-objective functions in the absence and presence of TCSC. It is observed that various parameters are reduced with TCSC placement at a particular location as compared to the without installation of TCSC. It is also noticed that the voltage profile is also improved.

Table 2. A contrast of FSI of the system for various weights.

m1(NLSI)	m2(NVSI)	Total FSI
0.5	0.5	7.3884
0.6	0.4	7.5503
0.7	0.3	7.7122
0.8	0.2	7.8741
0.9	0.1	8.036

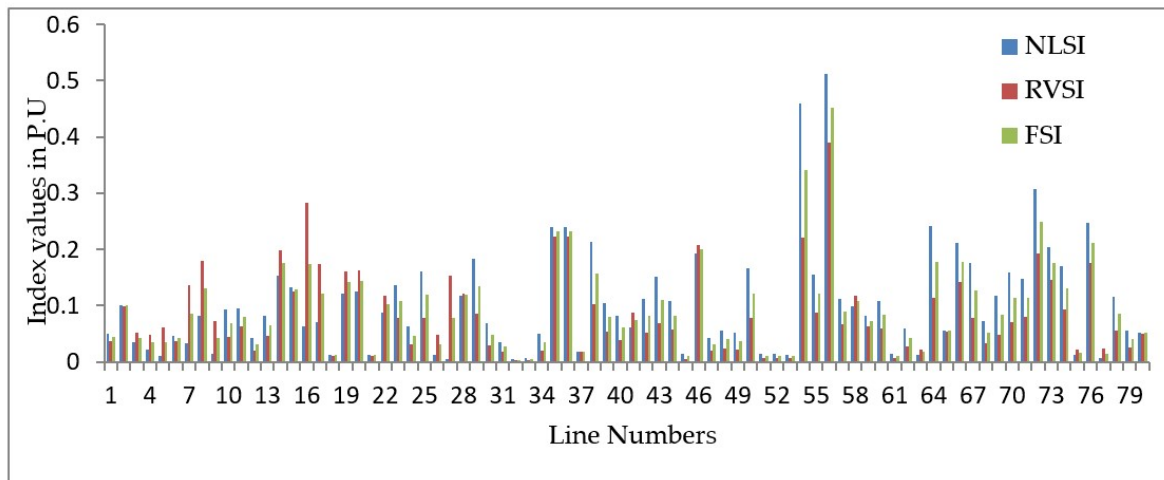


Figure 4. NLSI, RVSI and FSI values of all lines in IEEE-57-bus system.

Table 3. NLSI, RVSI and FSI Values of top 25 lines in IEEE-57-bus system.

LINE Numbers	SB Number	RB Number	NLSI (p.u.)	RVSI(p.u.)	FSI(p.u.)
56	41	43	0.5123	0.3905	0.4514
16	1	16	0.0633	0.2836	0.3404
35	24	25	0.2393	0.2235	0.2494
36	24	25	0.2393	0.2235	0.2314
54	11	41	0.4593	0.2214	0.2314
46	34	32	0.1923	0.2079	0.2119
14	13	15	0.154	0.1984	0.2001
72	44	45	0.3066	0.1922	0.1777
8	8	9	0.0812	0.1802	0.177
76	39	57	0.2469	0.1768	0.1762
17	1	17	0.071	0.1735	0.175
20	4	18	0.1249	0.162	0.1734
19	4	18	0.1223	0.1618	0.1575
27	12	17	0.0041	0.1535	0.1435
73	40	56	0.2046	0.1453	0.1421
66	13	49	0.2116	0.1423	0.1349
7	6	8	0.0339	0.1359	0.1313
15	1	15	0.1322	0.1244	0.1307
28	1	15	0.1169	0.1213	0.1283
58	15	45	0.0984	0.1181	0.1267
22	7	8	0.0881	0.117	0.1223
64	50	51	0.2413	0.1141	0.1223
38	26	27	0.2128	0.1023	0.1221
2	2	3	0.1011	0.0991	0.1194

Table 4. Multi-objective function in IEEE 57 bus system by locating TCSC in different places.

SB Number	RB Number	Total Power Generation (MW)	Fuel Cost (\$/h)	Active Power Losses(MW)	Emission(t/h)	Voltage Deviation in p.u	Valve Point Effect (\$/h)	Multi-Objective Function
41	43	1227.2	27487	31.41	1.0064	4.852	27534	11012
11	41	12274	27521	31.5975	1.0457	4.8338	27558	11023
13	15	12279	27515	32.0767	1.0593	4.912	27557	11022
44	45	12278	27485	31.955	1.0276	4.9304	27540	11013
50	51	1227.3	27489	31.1877	1.0065	4.8526	27537	11014

Table 5. Optimal Power flow solution without contingency using GWO.

Parameter		OF1	OF2	OF3	OF4	OF5	OF6
Real power generation (MW)	PG1(MW)	158.0297	265.076	163.4177	179.0372	170.1787	165.5765
	PG2(MW)	100	12.8868	100	100	100	100
	PG3(MW)	49.4902	125.903	49.9138	140	140	51.4046
	PG6(MW)	18.184	106.128	15.7625	150	150	14.9543
	PG8(MW)	490.8169	301.122	487.1829	243.1543	251.931	484.1597
	PGs(MW)	200	200	200	200	200	200
	PGw(MW)	210	210	210	210	210	210
Total Active power generation (MW)		1226.521	1221.12	1226.2769	1222.192	1222.11	1226.095
Total real power generation cost (\$/h)		27343	31769	27347	32907	32762	27352
Active power Loss (MW)		30.72	25.316	30.47	26.39	26.31	30.29
Valve point effect cost (\$/h)		27393	31815	27391	32946	32799	27393
Voltage deviation (p.u.)		4.9058	4.7912	4.8996	4.76	4.8	4.8951
Carbon Emission(ton/h)		1.0159	0.7945	1.0124	0.5924	0.5911	1.0479
Objective function		27343	25.316	27391	4.76	0.5911	10956
Computation time		27.99	26.99	23.68	23.98	22.76	23.44

OF1: Generation cost, OF2: Active power Loss, OF3: Valve point effect cost, OF4: Voltage Deviation, OF5: Carbon emissions, OF6: Multiobjective function.

Table 6. Optimal Power flow solution without contingency with TCSC using GWO.

Parameter		OF1	OF2	OF3	OF4	OF5	OF6
Real power generation (MW)	PG1(MW)	171.6265	265.1003	176.1099	324.9398	174.6181	184.4858
	PG2(MW)	100	29.0587	100	100	100	100
	PG3(MW)	47.3295	92.2253	47.8758	22.3223	140	48.5226
	PG6(MW)	16.8781	114.2285	12.0639	52.221	158.7316	6.2416
	PG8(MW)	479.7787	309.8535	479.4983	314.4824	239.0236	476.0984
	PGs(MW)	200	200	200	200	200	200
	PGw(MW)	210	210	210	210	210	210
Total Active power generation (MW)		1225.613	1220.466	1225.548	1223.966	1222.373	1225.348
Total real power generation cost (\$/h)		26580	30032	26582	30423	32409	26603
Active power Loss (MW)		29.812	24.66	29.74	28.165	26.57	29.5484
Valve point effect(\$/h)		26629	30070	26626	30461	32444	26635
Voltage deviation (p.u.)		4.8267	4.794	4.8247	4.7794	4.808	4.8206
Carbon Emission(ton/h)		0.9666	0.7936	0.9727	0.9524	0.5562	0.9755
Objective function		26580	24.66	26626	4.7794	0.5562	10655
Computation time(secs)		26.76	25.84	24.43	21.64	25.26	27.41

6.3. Contingency Condition using Intermittent Approach

The above system is also tested under contingency conditions using an intermittent method. The intermittent approach can be explained as the maximum value of FSI obtained during the line outages, multiplied by the number of times the probability of occurrence of the severity occurs in that line and is displayed in Figure 5. After the execution of contingency analysis, the intermittent severity index value can be determined to find out the better location for the placement of TCSC. Initially, the maximum value of the fused severity index among all the line outages is determined. Then the number of times that line was affected is determined. The line with the highest value of the line outage is multiplied by the number of times the line has been repeated for many line outages is taken as reference. It is noticed from Table 7 that line number 56 is the most severe line that is associated with buses no. 41–43 causes more stress on the line. This line 56 is removed and the load flow is done using Newton Raphson, this in turn gives the maximum severity value for line number 54, connected between buses 11–41, and hence TCSC is placed in line 54 under contingency conditions. This method provides a more accurate stressed line of the system as compared to the traditional way. The obtained maximum fused severity index values for distinctive line outages are represented as a stem plot shown in Figure 6. The box plot for (n-1) contingency of the modified IEEE 57 bus system is shown in Figure 7. The box plot shows all the FSI values taken for various line outages with maximum, minimum and median values. Table 8 gives the values for different parameters like own generators, real power generation, Active power loss, voltage deviation have been compared including and excluding contingency and TCSC. It is also further tuned with the grey wolf algorithm. Figure 8

indicates a marked improvement in the voltage profile of all buses without and with tuned TCSC under normal and contingency conditions. Tables 9 and 10 consist of different objective functions in the presence and absence of TCSC with contingency. As compared to the Table 9 the objectives functions such as total generation cost, valve-point loading effect, voltage deviation, carbon-emission, active power loss present in Table 10 gave better results with optimal placement of TCSC using the grey wolf technique. The value of the individual objective function and multi-objective function effectively decreased with optimal placement of TCSC and enhanced the power transfer capability of the electrical network. It shows that the proposed grey wolf technique gives better results. Table A1 depicts the characteristics of the IEEE-57 bus system and cost coefficients of solar and wind are taken as 1.5\$/h. Figure A1. Shows Integrated IEEE57 bus system with solar and wind

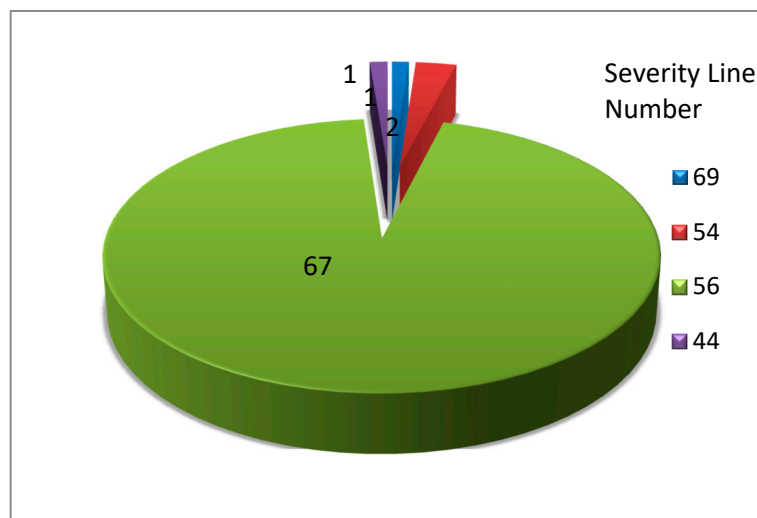


Figure 5. Probability of occurrence severity lines in IEEE-57-bus system.

Table 7. Contingency analysis by intermittent approach.

(Max FSI) x(No of Times the Severity of the Line)	Intermittent Index Value(p.u)	Severity Line No.	SB	RB
0.508323	0.508323	69	53	54
0.6100*2	1.22	54	11	41
0.614*67	41.138	56	41	43
0.537543	0.537543	44	31	32

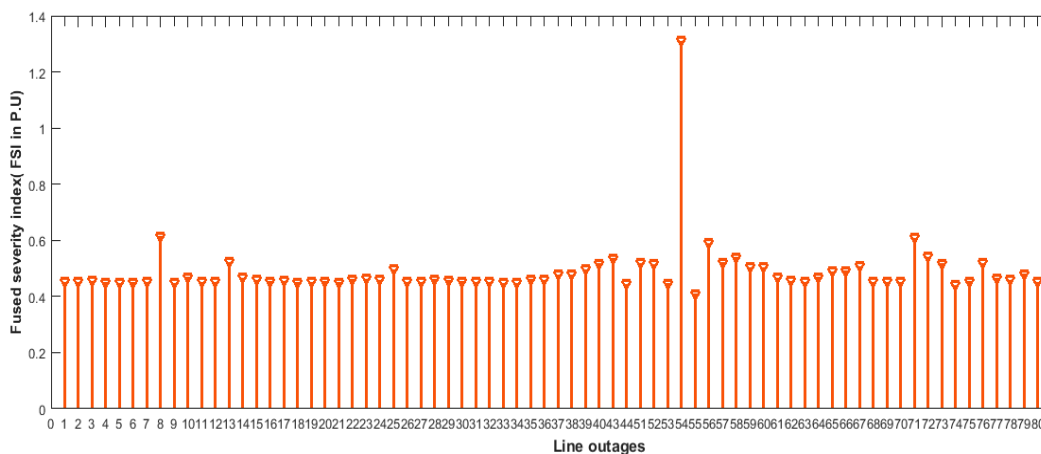


Figure 6. Maximum fused severity index values for various line outages.

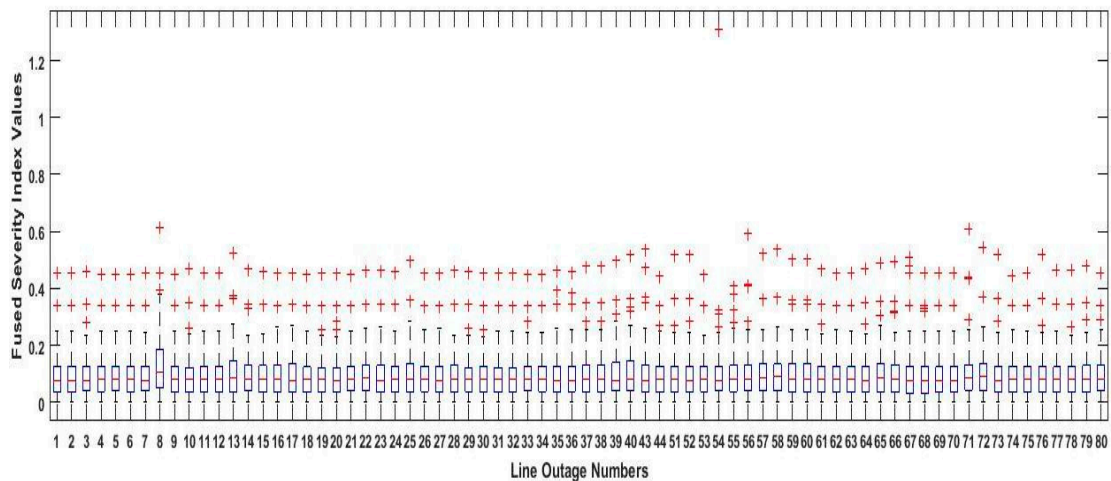


Figure 7. Box plot for fused severity index values for various line outages.

Table 8. Different parameters for the IEEE57bus system using the grey wolf algorithm.

Quantity	Tuned Without Contingency and TCSC	Tuned Without Contingency and with TCSC	Tuned with Contingency and without TCSC	Tuned with Contingency and TCSC	
Real power generation (MW)	P_{G1} (MW)	165.576	184.4858	152.2136	192.0006
	P_{G2} (MW)	100	100	100	100
	P_{G3} (MW)	51.4046	48.5226	49.3313	47.9692
	P_{G6} (MW)	14.9543	6.2416	16.5164	13.7667
	P_{G8} (MW)	484.159	476.0984	501.8825	464.311
	P_{Gs} (MW)	200	200	200	200
	P_{Gw} (MW)	210	210	210	210
Total power generation (MW)	1226.09	1225.35	1229.944	1228.048	
Total Load(MW)	1195.8	1195.8	1195.8	1195.8	
Active power Loss (MW)	30.29	25.62	34.1438	32.2475	
Voltage deviation (p.u.)	4.8951	4.77	6.1709	6.1562	

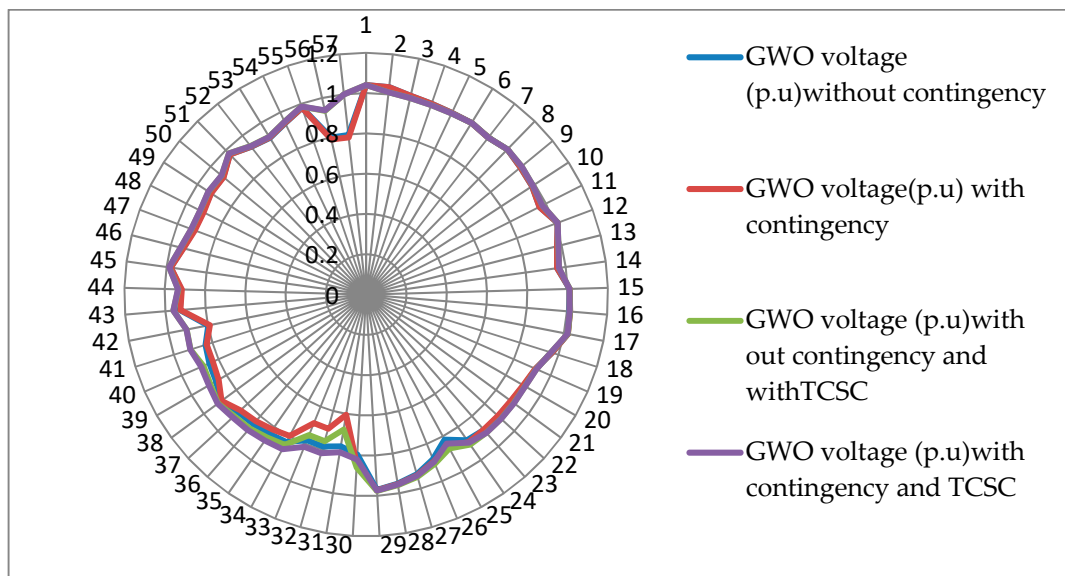


Figure 8. Voltage profile for the IEEE 57 bus system including and excluding TCSC.

Table 9. Optimal power flow solution with contingency using GWO.

Parameter		OF1	OF2	OF3	OF4	OF5	OF6
Real power generation (MW)	P_{G1} (MW)	160.8007	253.576	164.1703	236.6245	164.3258	152.2136
	P_{G2} (MW)	100	9.0711	100	100	100	100
	P_{G3} (MW)	50.0324	140	51.0861	140	140	49.3313
	P_{G6} (MW)	16.8994	103.6872	17.9614	3.989	150	16.5164
	P_{G8} (MW)	491.5837	307.4762	485.7775	335.7361	260.4213	501.8825
	P_{Gs} (MW)	200	200	200	200	200	200
	P_{Gw} (MW)	210	210	210	210	210	210
TotalActivepowergeneration (MW)		1229.316	1223.811	1228.995	1226.35	1224.747	1229.944
Total real power generation cost (\$/h)		27467	32206	27471	30867	3276	27472
Active power Loss (MW)		33.51	28.01	33.19	30.54	28.94	34.1438
Valve point effect(\$/h)		27516	32235	27515	30909	32804	27529
Voltage deviation (p.u.)		6.097	5.962	6.09	5.9411	5.9456	6.1109
Carbon Emission(t/h)		1.0233	0.7879	1.0096	0.7953	0.5958	1.0449
Objective function		27467	28.01	27515	5.9411	0.5958	11008
Computation time(s)		26.13	27.7	29.2	26.89	27.01	24.01

Table 10. Optimal power flowsolution with contingency and TCSC using GWO.

Parameter		OF1	OF2	OF3	OF4	OF5	OF6
Real power generation (MW)	P_{G1} (MW)	154.0963	269.203	156.1643	329.2276	158.5345	172.0006
	P_{G2} (MW)	100	29.692	100	100	100	100
	P_{G3} (MW)	47.7644	95.2386	48.1194	21.1564	140	47.9692
	P_{G6} (MW)	36.5722	115.8249	34.2858	52.4674	158.6377	13.7667
	P_{G8} (MW)	480.4047	303.6558	480.2326	314.3568	238.3618	464.311
	P_{Gs} (MW)	200	200	200	200	200	200
	P_{Gw} (MW)	210	210	210	210	230	230
Total active power generation (MW)		1228.838	1223.614	1228.802	1227.208	1225.534	1228.048
Total real power generation cost (\$/h)		26719	30403	26721	30710	32555	26759
Active power Loss (MW)		33.03	27.814	33.0021	31.4082	29.73	32.2475
Valve point effect(\$/h)		26767	30449	26765	30744	32588	26795
Voltage deviation (p.u.)		6.1681	6.1303	6.167	6.1143	6.1474	6.1562
Carbon emission(ton/h)		0.9728	0.7962	0.9755	0.9674	0.5614	0.95
Objective function		26719	27.814	26765	6.1143	0.5614	10719
Computation time(secs)		27.68	23.92	26.104	25.09	25.98	22.89

7. Conclusions

For any consistent and successful operation of integrated system generator reallocation, reducing the losses voltage and stability are the primary issues. A multi-objective function comprised of active power loss, generation fuel cost along with valve-point impact, voltage deviation carbon discharges, with the utilization of minimum value of TCSC is considered for the optimal tuning of TCSC using grey wolf optimization.

- A fused severity index has been implemented for finding out the most stressed line of the transmission system. The weak lines are recognized based on the rank and arranged in descending order of fused severity index for the lines associated between the buses.
- Uncertainties of solar and wind are demonstrated as lognormal and Weibull probabilistic distribution functions and their interconnections to the traditional grid are explained.
- The TCSC and output of generators are additionally tuned by limiting a multi-objective function comprising of active power loss, fuel cost with valve-point effect, carbon discharges utilizing grey wolf algorithm and the best global ideal values are achieved.
- A reduction in the losses, carbon discharges, fuel cost with valve-point effect has been obtained with an improvement in the voltage profile of the integrated system. The reduction in active power loss helps in contingency management. Improvement of voltage deviation helps in protecting the system against line outages.
- Finally, it can be inferred that the explored strategy is more capable in decreasing the losses, carbon emission and improving the voltage profile.

Author Contributions: Investigation, M.R.; Supervision, G.V.N.K. and S.S.

Funding: This research received no external funding.

Conflicts of Interest: The authors declare no conflict of interest.

Abbreviations

Nomenclature

TCSC	Thyristor-Controlled Series Compensator
SB	Sending end bus
RB	Receiving end bus
RVSI	Rapid Voltage Stability Index
NLSI	Novel Line Stability Index
FSI	Fused Severity Index.
PDF	Probability Density Function
GWO	Grey Wolf Optimizer
FACTS	Flexible AC Transmission System
VD	Voltage Deviation
VPE	Valve Point Effect
CE	Carbon Emissions
IMSI	Intermittent Severity Index
OPF	Optimal Power Flow
PV	Photo Voltaic
SVC	Static VAR Compensator

Symbols

P_{we}	Wind power generation from eth bus
P_{sf}	Power output from the fth PV plant
P_L	Overall real power loss
Q_L	Overall reactive power loss,
P_{Gi}	Real power generated in ith bus
P_{Di}	Real power demanded in ithbus
P_{TGI}^{\min}	The minimum power of the ith thermal unit
P_j	Active power at receiving at jth bus
Q_j	Reactive power at receiving at jth bus
N_{TG}	Number of generator buses
a, b, c	Fuel cost coefficients
V_k	Magnitude of voltage at bus k
X	Reactance of line
X_{TCSC}	Reactance of the TCSC
V_{in}	Wind Speed (Cut-in)
V_{CO}	Wind Speed (Cut-out)
V_r	Wind Speed (Rated)
P_r	Rated Power
n_{tl}	No. of lines for transmission
N	no of buses
Z	impedance of line in ohms
g_e	Direct cost coefficient of the eth wind farm
h_f	Direct cost coefficient of the fth solar plant
R_{ij}	The resistance of the line
S_{ij}	Apparent power flowing in the line
V_{kref}	Magnitude of the Reference voltage at the busk
d_i, ϵ_i	Valve-Point Effect Coefficient
$\delta_i, \varphi_i, \lambda_i, \psi_i, \sigma_i$	Emission coefficients
c	Scale Parameter

k	Shape Parameter
PB_{ij}	Probability occurring of line ij for all contingencies of the system
B	variance of the lognormal distribution
μ	Mean of the lognormal distribution
$w_1, w_2, w_3, w_4, w_5, m_1, m_2$	Weighted factors

Appendix A

Table A1. Generator Characteristics of IEEE 57 Bus Systems.

Generator Bus No.	a (\$/MW ² /h)	b (\$/MW/h)	c (\$/h)	P_G^{min} (MW)	P_G^{max} (MW)	δ_i	φ_i	λ_i	ψ_i	σ_i	di	ei
1	0.0775	20	0	0	1975	4.091	-5.55	0.549	0.0002	0.286	18	0.037
2	0.01	40	0	0	100	2.543	-6.04	0.4638	0.0005	0.333	16	0.038
3	0.25	20	0	0	140	6.131	-5.55	0.4151	0.00001	0.667	13.5	0.041
6	0.1	40	0	0	100	3.491	-5.75	0.539	0.0003	0.266	18	0.037
8	0.02222	20	0	0	550	4.258	-5.09	0.3586	0.000001	0.8	14	0.04

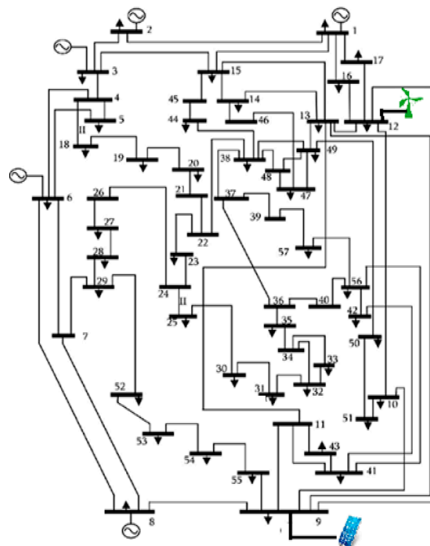


Figure A1. Integrated IEEE57 bus system with solar and wind.

References

- Ogunjuyigbe, A.S.O.; Ayodele, T.R.; Akinola, O.A. Optimal allocation and sizing of PV/Wind/Split-diesel/Battery hybrid energy system for minimizing life cycle cost, carbon emission and dump energy of the remote residential building. *Appl. Energy* **2016**, *171*, 153–171. [[CrossRef](#)]
- Kusakana, K. Optimal scheduled power flow for distributed photovoltaic/wind/diesel generators with battery storage system. *IET Renew Power Gener.* **2015**, *9*, 916–924. [[CrossRef](#)]
- Sanseverino, E.R.; Di Silvestre, M.L.; Badalamenti, R.; Nguyen, N.Q.; Guerrero, J.M.; Meng, L. Optimal power flow in islanded microgrids using a simple distributed algorithm. *Energies* **2015**, *8*, 11493–11514. [[CrossRef](#)]
- Erdinc, O.; Uzunoglu, M. Optimum design of hybrid renewable energy systems: Overview of different approaches. *Renew Sustain. Energy Rev.* **2012**, *16*, 1412–1425. [[CrossRef](#)]
- Deng, W.; Zhang, B.; Ding, H.; Li, H. Risk-based probabilistic voltage stability assessment in an uncertain power system. *Energies* **2017**, *10*, 180. [[CrossRef](#)]
- Shadmand, M.B.; Balog, R.S. Multi-objective optimization and design of a photovoltaic-wind hybrid system for community smart DC microgrid. *IEEE Trans. Smart Grid* **2014**, *5*. [[CrossRef](#)]
- Rambabu, M.; Nagesh Kumar, G.V.; Siva Nagaraju, S. Energy management of microgrid using support vector machine (SVM) model. *IIOAB J.* **2016**, *7*, 116–132.
- Carvalho, J.P.; Shaw, B.J.; Avila, N.I.; Kammen, D.M. Sustainable Low-Carbon Expansion for the Power Sector of an Emerging Economy: The Case of Kenya. *Environ. Sci. Technol.* **2017**, *51*, 10232–10242. [[CrossRef](#)]

9. Abaci, K.; Yamacli, V. Differential search algorithm for solving multi-objective optimal power flow problem. *Int. J. Electr. Power Energy Syst.* **2016**, *79*, 1–10. [[CrossRef](#)]
10. Shi, L.; Wang, C.; Yao, L.; Ni, Y.; Bazargan, M. Optimal power flow solution incorporating wind power. *IEEE Syst. J.* **2012**, *6*, 233–241. [[CrossRef](#)]
11. Sichilalu, S.; Mathaba, T.; Xia, X. Optimal control of a wind–PV-hybrid powered heat pump water heater. *Appl. Energy* **2017**, *185*, 1173–1184. [[CrossRef](#)]
12. Levron, Y.; Guerrero, J.M.; Beck, Y. Optimal Power Flow in Microgrids With Energy Storage. *Power Syst. IEEE Trans.* **2013**, *PP*, 1–9. [[CrossRef](#)]
13. Biswas, P.P.; Suganthan, P.N.; Amaratunga, G.A.J. Optimal power flow solutions incorporating stochastic wind and solar power. *Energy Convers. Manag.* **2017**, *148*, 1194–1207. [[CrossRef](#)]
14. HamzehAghdam, F.; Salehi, J.; Ghaemi, S. Contingency based energy management of multi-microgrid based distribution network. *Sustain. Cities Soc.* **2018**, *41*, 265–274. [[CrossRef](#)]
15. Rao, V.B.; Engineering, E.; Kumar, G.V.N.; Engineering, E. A Comparative Study of BAT and Firefly Algorithms for Optimal Placement and Sizing of Static VAR Compensator for Enhancement of Voltage Stability. *Int. J. Energy Optim. Eng.* **2015**, *4*, 68–84. [[CrossRef](#)]
16. Hingorani, N.G.; Gyugyi, L.; El-Hawary, M. *Understanding FACTS—Concepts and Technology of Flexible AC Transmission Systems*; Wiley-IEEE Press: Hoboken, NJ, USA, December 1999.
17. Bali, S.K.; Munagala, S.; Gundavarapu, V.N.K. Harmony search algorithm and combined index-based optimal reallocation of generators in a deregulated power system. *Neural Comput. Appl.* **2017**, 1–9. [[CrossRef](#)]
18. Kumar Gundavarapu, V.N.; Mishra, A. Line utilization factor-based optimal allocation of IPFC and sizing using firefly algorithm for congestion management. *IET Gener. Transm. Distrib.* **2016**, *10*, 115–122. [[CrossRef](#)]
19. Modarresi, J.; Gholipour, E.; Khodabakhshian, A. A comprehensive review of the voltage stability indices. *Renew Sustain. Energy Rev.* **2016**, *63*, 1–12. [[CrossRef](#)]
20. Kim, S.S.; Kim, M.K.; Park, J.K. Consideration of multiple uncertainties for evaluation of available transfer capability using fuzzy continuation power flow. *Int. J. Electr. Power Energy Syst.* **2008**, *30*, 581–593. [[CrossRef](#)]
21. Nireekshana, T.; KesavaRao, G.; SivanagaRaju, S. Available transfer capability enhancement with FACTS using Cat Swarm Optimization. *Ain Shams Eng. J.* **2016**, *7*, 159–167. [[CrossRef](#)]
22. Samimi, A.; Naderi, P. A New Method for Optimal Placement of TCSC Based on Sensitivity Analysis for Congestion Management. *Smart Grid Renew. Energy* **2012**, *2012*, 10–16. [[CrossRef](#)]
23. Bhattacharyya, B.; Gupta, V.K. SVC & TCSC for Minimum Operational Cost Under Different Loading Condition. 2012, pp. 1–6. Available online: www.iitk.ac.in/npsc/Papers/NPSC2012/papers/12055.pdf. (accessed on 26 June 2018).
24. Mukherjee, A.; Mukherjee, V. Solution of optimal power flow using chaotic krill herd algorithm. *Chaos Solit. Fract.* **2015**, *78*. [[CrossRef](#)]
25. Vlachogiannis, J.G.; Lee, K.Y. A comparative study on particle swarm optimization for optimal steady-state performance of power systems. *IEEE Trans. Power Syst.* **2006**, *21*, 1718–1728. [[CrossRef](#)]
26. Daryani, N.; Hagh, M.T.; Teimourzadeh, S. Adaptive group search optimization algorithm for multi-objective optimal power flow problem. *Appl. Soft Comput. J.* **2016**, *38*, 1012–1024. [[CrossRef](#)]
27. Mirjalili, S.; Mirjalili, S.M.; Lewis, A. Grey Wolf Optimizer. *Adv. Eng. Softw.* **2014**, *69*, 46–61. [[CrossRef](#)]
28. Murty, V.V.S.N.; Kumar, A. Optimal placement of DG in radial distribution systems based on new voltage stability index under load growth. *Int. J. Electr. Power Energy Syst.* **2015**, *69*, 246–256. [[CrossRef](#)]
29. Yazdanpanah-Goharrizi, A.; Asghari, R. A Novel Line Stability Index (NLSI) for Voltage Stability assessment of Power Systems. In Proceedings of the 7th WSEAS e 7th WSEAS International Conference on Power Systems, Beijing, China, 15–17 September 2007; pp. 164–167.
30. Fort Collins Data Access: Results. Available online: http://climate.colostate.edu/~{autowx/fclwx_results.php (accessed on 26 June 2018).

